Algal Research 40 (2019) 101501

Contents lists available at ScienceDirect

Algal Research

journal homepage: www.elsevier.com/locate/algal

Simultaneous solid and biocrude product transformations from the hydrothermal treatment of high pH-induced flocculated algae at varying Ca concentrations

Robert D. Hable[a], Sirwan Alimoradi[b], Belinda S.M. Sturm[b], Susan M. Stagg-Williams[a,*]

[a] Chemical & Petroleum Engineering Department, The University of Kansas, Lawrence, KS 66045, USA
[b] Civil, Environmental, and Architectural Engineering Department, The University of Kansas, Lawrence, KS 66045, USA

ARTICLE INFO

Keywords:
Algae
Biofuels
Hydrothermal liquefaction
Phosphorus recovery
Calcium phosphate

ABSTRACT

Because of the substantially high growth rate, algae have become a prominent biomass feedstock to produce biofuels and renewable chemicals leading to research on cost-competitive means to cultivate and convert algal biomass. Wastewater effluent streams provide the necessary water and nutrient inputs for algal growth, however, the low lipid, high ash composition of algal solids produced are not ideal for conventional conversion techniques. Hydrothermal liquefaction (HTL) is a holistic algal conversion method that utilizes subcritical water to produce biocrude and high-valued solid product from wastewater-cultivated algal solids. The objective of this study was to understand how calcium, the primary inorganic element of wastewater-cultivated algal solids, affects the final HTL products. The calcium concentration was varied in six algal growth tanks and the algae was harvested *via* high pH induced-flocculation. The algal biomass was then processed using HTL at 350 °C for 1 h. Calcium carbonate was the primary crystalline structure observed in the algal and HTL solids. One HTL solid sample showed a significant production of tricalcium phosphate. The higher calcium concentrations resulted in near 100% capture of phosphorus in the HTL solids. Increasing the calcium content also had a positive impact on the biocrude including the H/C ratio, amide, alkene, and carboxylic acid content. The results of this study suggest that the inorganic solids collected from high pH, flocculated harvesting may have an *in-situ* catalytic impact on the biocrude.

1. Introduction

The effluent from municipal wastewater treatment facilities (WWTF) is a potential water and nutrient source for algal cultivation that is both sustainable and inexpensive. Algae can assimilate a majority of the remaining nitrogen (N) and phosphorus (P) from the effluent, thus inhibiting nutrient accumulation in lakes and river deltas [1,2]. However, algae cultivated from wastewater (WW) typically has a low lipid and high ash content [3–6], which is not ideal for lipid conversion to biofuels. Furthermore, algal lipid conversion technologies often require extensive drying and hazardous solvents. Hydrothermal liquefaction (HTL) is a thermochemical process that converts wet algal biomass to a biocrude product that is comparable to petroleum crude [7]. HTL requires subcritical temperatures and pressures (250–350 °C; 5–22 MPa) to produce the liquid, biocrude product, and by operating at 10–30 wt% solids, HTL greatly reduces the energy-intensive, dewatering step required for other algal conversion techniques [8–11].

We have previously reported [3,12] on HTL utilizing mixed-culture algae cultivated in WW, which resulted in different product yields than more commonly reported single-species, low-ash algae. Analysis of the HTL products from WW-cultivated algae revealed that the biocrude yields on an ash-free, dry-weight (afdw) basis are comparable to those of low-ash algae. However, high ash contents of the algae and subsequent higher HTL solids yields were observed. Further analysis of the algal and HTL solids revealed high levels of calcium, which was ascribed to the addition of lime, $Ca(OH)_2$, as a buffering agent to the WW treatment process. In addition to the higher solids yields, notable differences in the biocrude quality and composition, including higher carbon and lower nitrogen and oxygen recovery, were observed, suggesting *in-situ* catalytic upgrading of the biocrude occurred. Similar results have recently been reported by Chen, et al. [13]

Along with the higher levels of calcium observed, we have also reported that 95% of the phosphorus contained in the algal solids is recovered in the HTL solid product as a highly substituted hydroxyapatite

* Corresponding author at: Chemical & Petroleum Engineering, The University of Kansas, 4142 Learned Hall, 1530 W. 15th Street, Lawrence, KS 66045, USA.
E-mail address: smwilliams@ku.edu (S.M. Stagg-Williams).

https://doi.org/10.1016/j.algal.2019.101501
Received 31 December 2018; Received in revised form 8 April 2019; Accepted 8 April 2019

(HAp), $Ca_5(PO_4)_3OH$. This is in contrast to results from HTL of low ash algae in which high levels of phosphorus remain in the aqueous co-product (ACP) [14,15]. The presence of calcium in the wastewater algal solids was reported to play a role in the high P-recovery in the solid phase [12]. Others have observed similar impacts of inorganics on the phosphorus recovery. Yu, et al. [16] hypothesized that the calcium and magnesium content are pivotal in the fate of phosphorus in the HTL products, but only a 47% P-recovery in the solids was achieved when doping the HTL reaction with metal catalysts. High solid P-recovery, up to 89%, has also been observed at hydrothermal processing at lower temperature and pressures known as hydrothermal carbonization (HTC) where it has also been hypothesized that the metal:P ratio of the feedstock impacts the solid-P recovery [17].

The addition of metal cations such as Ca^{2+} and Mg^{2+} in the algal solids may benefit the recovery of P in the solid-phase post-HTL, but it also increases the amount of inorganics present with the algal biomass. The higher inorganic content in the algal feedstock solids results in higher HTL solids yields, but these solids may also have an *in-situ* catalytic impact on the biocrude product. The objective of this paper is to demonstrate the role that the Ca:P molar ratio in algal solids has on: 1) the fate of P post-HTL, 2) the structure of the HTL solids, and 3) the quality of biocrude produced. To the best of the author's knowledge, this is the first study where the inorganic content in the HTL reactor is varied by controlling algal growth conditions and harvesting techniques as opposed to doping the reactor with catalysts. In addition, this is the first study to examine the *in-situ* effects that solid synthesis may have on biocrude composition.

2. Experimental methods

2.1. Algal cultivation & characterization

Chlorella kessleri (UTEX 262) culture was inoculated in BG-11 nutrient media [18] in six, 15 L light rack tanks. The nitrogen to phosphorus molar ratio (N:P) was constant at 78, while $CaCl_2$ was added to adjust the theoretical Ca:P molar ratio in each tank. The pH remained neutral (7.0 ± 0.1) during growth by continually bubbling CO_2 into the tanks. Optical density measurements were used to monitor the growth stage of the algae using a spectrophotometer (5810R, Eppendorf,) at 600 nm wavelength [19].

Once the cultures reached the stationary phase, the pH in each tank was increased to 10.5 by adding caustic soda (2 M NaOH). The rise in pH caused a shift in the media equilibrium that benefited solid precipitation and algal flocculation [20,21]. Samples of the growth media were taken prior to inoculation (Pre-Growth), before increasing the pH (Pre-Floc), and after auto-flocculation was complete (Post-Floc). From these media samples the calcium (Ca), phosphorus (P), and magnesium (Mg) concentrations were measured in triplicate using a Varian 725-ES inductively coupled plasma-optical emission spectrometer (ICP-OES, Varian 725-ES, Varian, Australia). These elements are of interest as they have been previously reported to have a concentration > 1 mg/L in wastewater growth media and nearly 90% or higher recovery in the HTL solids [12]. Alkalinity and pH were also measured in the Pre-Floc and Post-Floc media to calculate total carbonate (CO_3^{2-}) before and after flocculation. Further dewatering of the algal slurry was done using an Eppendorf 5810R centrifuge at 12857*g* (RCF) for 2 min. Finally, the algal solids were freeze-dried in a Labconco Freezone 4.5 and ground to obtain a powder with < 5 wt% moisture.

After a low moisture powder was achieved, the algal solids were further characterized. Proximate analysis of the algal solids was conducted in triplicate by a Thermal Analysis Q600 Thermogravimetric Analyzer (TGA) (TA Instruments, New Castle, Pennsylvania, USA) using a previously described method [12]. An ultimate, CHN/O elemental analysis was measured in triplicate by a Perkin Elmer 2400 Series II Elemental Analyzer (Waltham, MA). The final inorganic content (mg/kg) of the algal solids for the elements of interest (Ca, P, and Mg) was calculated from the difference in concentrations between the Pre-Growth and Post-Floc media, while the final mass of algal solid biomass was determined after freeze-drying and grinding. To detect and define possible crystalline structures within the algal solids, a Bruker Micro-Star micro-focus rotating anode x-ray source at 45 kV and 60 mA was used with an APEX II CCD detector. The method for XRD diffraction has been previously reported [12].

To estimate the macromolecular contents of the algal solids, the Anthrone method [22] was used for measuring carbohydrate amount and the Lowry protein assay [23] estimated the protein content. A three-solvent lipid extraction technique was performed for straight lipid extraction. The solvent solution of hexane, tetrahydrofuran, and methylene chloride was prepared at a 1:1:1 by volume ratio [24]. To extract the lipids from the algal biomass, 5 mL aliquots of the solvent solution were added to 200 mg of dried algae mass and sonicated. The solid-liquid mixture was then centrifuged at 1159*g* (RCF) for 2 min and the supernatant was extracted. An additional 5 mL aliquot of the solvent solution then added to the residual solids and the previous process was repeated. This procedure was repeated thrice until a total of 15 mL of extracted lipids and solvent solution was obtained. The solvent solution was then evaporated off using nitrogen, and the residual lipids were processed into fatty acid methyl esters (FAMEs) *via* the transesterification method reported by Laurens et al. [25]. The resulting neutral lipid components were analyzed by gas chromatography mass spectrometry (GC/MS, 7890B, Agilent, Ltd., California, USA) to confirm complete conversion and to identify primary FAMEs within the algal biomass [26]. Ethyl stearate (Sigma Aldrich > 99%) was used as an internal standard to further quantify the amount of lipids in the algal sample.

2.2. Hydrothermal liquefaction & extraction procedure

Hydrothermal reactions were conducted in 75 mL, 4740 series Parr reactors. The reactors were loaded with 30 mL of DI water and 10 wt% freeze-dried algae. The algae and water were mixed until homogenous. Nitrogen was used to purge oxygen from the reactors. The reactors were heated using a Techne SBL-2D fluidized sand bath with a Techne TC-8D temperature controller from room temperature to 350 °C at 3 °C/min then held isothermally for 60 min. The reactors were immediately quenched with room temperature water and the gas vented. The ACP was collected first by pouring the reactor contents over a 2.5 µm filter and applying vacuum. The remaining reactor contents and vacuum filter were washed thoroughly with dichloromethane (DCM) and gravity filtered through an 8 µm filter. The DCM and dissolved biocrude were collected in a round-bottom flask. Finally, the DCM was distilled to < 5 wt% remaining in the biocrude product.

2.3. Yield and product characterization

Product yields for biocrude, HTL solids, and aqueous carbon were reported on a dry weight (dw) basis. The following equations were used to determine product yields:

$$\text{Biocrude Yield} = \frac{\text{wt}_{\text{biocrude}}(1 - \%\text{DCM})}{\text{algae}_{\text{dw}}} \times 100 \quad (1)$$

$$\text{Solids Yield} = \frac{\text{wt}_{\text{solids}} \times \%\text{ash}_{\text{solids}}}{\text{algae}_{\text{dw}}} \times 100 \quad (2)$$

$$\text{Aqueous Carbon} = \frac{\text{vol}_{\text{ACP}} \times \text{TOC}}{\text{algae}_{\text{dw}} \times \%\text{carbon}_{\text{dw}}} \times 100 \quad (3)$$

where algae_{dw} is the dry weight mass of algal solids loaded into the reactor; $\text{wt}_{\text{biocrude}}$ is the measured biocrude mass after distillation; % DCM is the weight percent of DCM remaining in the biocrude after distillation; $\text{wt}_{\text{solids}}$ is the total mass of dry HTL solids after gravity and vacuum filtration; $\%\text{ash}_{\text{solids}}$ is the ash weight percent of the HTL solid

product; vol_{ACP} is the measured volume of ACP after vacuum filtration; TOC is the measured concentration of organic carbon in the ACP; and % $carbon_{dw}$ is the dry weight percentage of carbon in the algal solids. The amount of biomass generated in this study only allowed for single HTL reactions to be conducted. Triplicate HTL reactions in the identical 75-mL reactors were performed on wastewater algal solids of similar dry weight composition. Biocrude yields (dw%) of 19.9, 20.2 and 19.5 and HTL solid yields (dw%) of 24.5, 25.4 and 25.0 were obtained. The uncertainty for the biocrude and HTL solid yields was 0.4 dw% and 0.5 dw%, respectively. We expect the reactions in this study to have similar uncertainties.

Ultimate analysis of the biocrude was also determined in triplicate by a Perkin Elmer 2400 Elemental Analyzer from which the estimated energy density, or higher heating value (HHV), of the biocrude was calculated by the Dulong formula seen in Eq. 4).

$$HHV\ (MJ/kg) = 0.338\ wt\%C + 1.428 wt\%H - 0.1785 wt\%O \quad (4)$$

The remaining DCM solvent amount as well as the various oil fractions present in the biocrude were determined using a Thermal Analysis Q600 TGA using a previously reported simulated distillation (SimDist) method [12]. Lastly, gas chromatography–mass spectrometry (GC–MS) was performed on the biocrude using an Agilent 7890 Series GC system with an Agilent HP-5MS UI column (30 m length; 0.25 mm diameter; and 0.25 μm thickness). The biocrude sample preparation and injection method are identical to what has previously been reported [12].

The HTL solids product were characterized similarly to the algal solids. The ash content and the crystalline structure of the HTL solids were determined using the same proximate analysis and XRD methods described for the algal solids. Carbonate wt% for the HTL solids was also determined by TGA, as the derivative weight (wt%/min) that appears between 600 and 800 °C. This is supported from the CO_3^{2-} balance on the Pre- and Post-Floc media, the experimental testing on pure $CaCO_3$, and from the literature that states CO_2 is liberated from $CaCO_3$ at these temperature ranges to form CaO [27]. Thus, a wt% CO_3 could be calculated from the wt% CO_2 loss from the TGA proximate analysis. Additionally, Fourier Transform Infrared Spectroscopy (FTIR) was performed on the HTL solids from a Varian 640-IR equipped with a GladiATR (PIKE Technologies). Due to limited formation of HTL solid product a single XRD, FTIR, and TGA analysis was performed. Finally, total organic carbon (TOC) and total nitrogen (TN) of the ACP were measured in triplicate using a Teledyne Tekmar TORCH TOC/TN Analyzer (Teledyne Tekmar, Waltham, MA), while the inorganic content was measured by ICP-OES. The inorganic species content of the HTL solids was calculated from the balance of the inorganics loaded with the algal solids and the measured inorganic concentrations and volumes in the ACP. It was assumed that negligible amounts of the inorganic species of interest: Ca, P, and Mg could be found in the biocrude product [28].

3. Results & discussion

3.1. Algal solid characterization

Table 1 displays the measured calcium, phosphorus, and magnesium concentrations for the Pre-Growth, Pre-Floc, and Post-Floc media. The magnesium concentration in the Pre-Growth media was constant across all six tanks at 7 mg/L. As intended, the calcium concentration in the Pre-Growth media increased from 9.2 to 57.2 mg/L from tanks 1 to 6 respectively. The phosphorus concentration gradually decreased from 7.0 to 5.5 mg/L from tanks 1 to 6 respectively in the Pre-Growth media. The lower phosphorus concentrations were most likely due to the substantial increases of Ca in these tanks causing some calcium phosphate to precipitate out of solution. Overall, the Pre-Growth media Ca:P molar ratio ranged from 1.0 to 8.0.

After the algae had reached the stationary growth stage, the phosphorus remaining in the Pre-Floc media was < 1 ppm in all six tanks. This large decrease in phosphorus concentration is due to the limiting phosphorus growth conditions and phosphorus assimilation to construct biomolecular components such as DNA, ATP, and phospholipids. Magnesium is also assimilated into the cell which can explain a reduction of approximately 2 mg/L of magnesium between Pre-Growth and Pre-Floc media. With the exception of tank 1, the calcium concentration increased from 1.5 mg/L to as much as 8 mg/L in tanks 4 and 5 between Pre-Growth and Pre-Floc measurements. This rise in calcium concentration can be explained from the approximately two liters of water lost to evaporation in the individual tanks between Pre-Growth and Pre-Floc.

After high-pH flocculation, a decrease in concentration was observed for the three dominant inorganic elements. Except for tank 1, most of the remaining calcium in the Pre-Floc media (> 60%) precipitated from solution. The phosphorus concentration also decreased between the Pre- and Post-Flocc media. However, due to its initial low concentration in the Pre-Floc media, only minimal amounts of phosphorus could have precipitated. Finally, the magnesium concentration decreased approximately 2 mg/L across all six tanks after flocculation at a high pH. Vandamme, et al. [29] demonstrated that the presence of soluble calcium and magnesium increased the flocculation efficiency of *Chlorella vulgaris* at pH between 10.5 and 12.

Table 2 describes the proximate analysis and inorganic content of the algal solids harvested from each of the six tanks. The combustible (comb.) wt% of the six algal solids were generally the same, ranging from 15 to 18 wt%. Algal solids harvested from tanks 1–3 had approximately 75–76 wt% volatile material, while tanks 4–6 were slightly lower at 68–72 wt%. As expected, higher calcium concentrations and ash contents were observed in the algal solids harvested from tanks 4–6 compared to the growth tanks with lower calcium contents in the Pre-Growth media. The calculated calcium concentrations increased from near 2500 mg/kg to over 100,000 mg/kg, while the ash content increased from near 6 wt% to almost 13 wt%. Finally, the total phosphorus content of the algal solids was slightly higher in tanks 1–3 (12,000–14,000 mg/kg) compared to tanks 4–6 (10,000–11,000 mg/kg). Meanwhile, the magnesium content was more scattered with algal solids from tank 3 having the most Mg (12,380 mg/kg) and tank 4 the least (7780 mg/kg). The remainder of algal solids had between 8000 and 9000 mg/kg of Mg.

As calcium increased in the algal solids, so did the carbonate (CO_3) wt%. The amount of carbonate that precipitated out during harvesting can be calculated based on the alkalinity (CO_3^{2-}), and the Ca^{2+} and PO_4^{3-} concentration of media. Previous studies calculating saturation indexes for different calcium species have shown that hydroxyapatite is a thermodynamically stable species [30]. In a chemically defined aqueous solution containing calcium and carbonate, $CaCO_3$ can be a dominant precipitant when the PO_4^{3-} is low at an elevated pH. XRD patterns of the algal solids harvested from tanks 4–6 confirmed the presence of calcite ($CaCO_3$). Although the XRD patterns of the algal solids harvested from tanks 1–3 were amorphous, the calculations at the alkalinity and pH during harvesting in this study still suggest $CaCO_3$ precipitation during high-pH flocculation.

The ultimate and macromolecular content of the algal solids harvested from each tank is shown in Table 3. Tanks 4–6 had a lower dry weight percentage (dw%) carbon, hydrogen, and nitrogen (avg. 48.3, 6.1, and 7.8 dw% respectively) than tanks 1–3 (avg. 53.6, 6.9, and 9.0 dw%), while the oxygen content remained constant near 20 dw%. Lower carbohydrate, lipid, and protein contents were also observed in tanks 4–6. The macromolecular content of algal biomass is related to the initial N:P ratio of the growth media and growth phase at the time of harvesting [31–33]. While both these parameters were constant in this study, the initial loss of phosphorus presumed to be due to calcium phosphate precipitation in the Pre-Growth media, is likely the cause of the differences in the ultimate and biochemical contents between tanks 1–3 and tanks 4–6.

Table 1
Inorganic concentrations of the six individual light rack tanks before inoculation (Pre-growth), upon reaching stationary phase and before auto-flocculation (Pre-Floc), and the supernatant after auto-flocculation (Post-Floc). Non-detectable (n.d.) is < 0.05 mg/L. (n.a) represents a single measurement.

Tank	Pre-Growth				Pre-Floc				Post-Floc		
	Ca	P	Mg	Ca:P	Ca	P	Mg	Alkalinity	Ca	P	Mg
	mg/L	mg/L	mg/L	mol	mg/L	mg/L	mg/L	mg/L as $CaCO_3$	mg/L	mg/L	mg/L
1	9.2 ± 0.1	7.0 ± 0.1	7.7 ± 0.1	1.0	9.1 ± 0.1	0.6 ± 0.1	5.6 ± 0.1	249 ± 2	9.3 ± 0.1	0.5 ± 0.1	4.4 ± 0.1
2	19.0 ± 0.1	6.5 ± 0.1	7.3 ± 0.1	2.3	20.5 ± 0.1	0.2 ± 0.1	5.5 ± 0.1	359 ± 4	7.7 ± 0.1	0.1 ± 0.1	3.5 ± 0.1
3	28.8 ± 0.2	6.1 ± 0.1	7.4 ± 0.2	3.7	31.2 ± 0.1	0.2 ± 0.1	5.4 ± 0.1	363 ± 5	5.3 ± 0.1	n.d.	1.7 ± 0.1
4	38.0 ± 0.1	6.0 ± 0.1	7.3 ± 0.2	4.9	46.0 ± 0.1	0.7 ± 0.1	5.8 ± 0.1	410 ± 2	14.1 ± 0.1	0.3 ± 0.1	3.9 ± 0.1
5	44.5 ± 0.2	5.9 ± 0.1	7.2 ± 0.2	5.9	52.7 ± 0.1	0.1 ± 0.1	5.2 ± 0.1	410 ± 2	4.2 ± 0.1	n.d.	2.6 ± 0.1
6	57.2 ± 0.3	5.5 ± 0.1	7.3 ± 0.1	8.0	63.4 ± 0.2	n.d.	5.3 ± 0.1	391 (n.a)	4.2 ± 0.1	n.d.	3.6 ± 0.1
		$n = 3$				$n = 3$		$n = 2$		$n = 3$	

It should be noted that the mass balance from the ultimate analysis, on an ash-free, dry weight (afdw%) basis, was within 7% for the algae harvested from all six tanks. Similarly, the afdw% balance for the algae harvested from tanks 1–3 was within 6%. However, for the algae harvested from tanks 4–6 the afdw% balance had a discrepancy between 8% and 23%. The difference can be explained by the presence of carbonate in the algal solids leading to an underestimation of the ash wt% with TGA. During the pyrolysis and combustion of the algal solids containing high levels of carbonate, carbon dioxide is produced. This carbon dioxide is associated with the decomposition of carbonate and would not be accounted for by conventional methods to measure protein, carbohydrates, and lipids. When the mass due to CO_2 loss is incorporated in the afdw%, the balance, the material balance is consistent for the algae harvested from all six tanks.

3.2. HTL product yields and recovery

Fig. 1 reports the biocrude and solid product yields from conventional HTL of the algal solids harvested from each tank. The highest and lowest biocrude yields on a dry weight basis were 47.8 dw% observed with algal solids from tank 2 and 35.4 dw% produced by algal solids harvested from tank 5. The biocrude yield on an ash free dry weight basis ranged from 35 to 45 afdw%. These biocrude yields for conventional HTL are consistent with the previous studies reported in the literature [3,9,12,34]. As expected, the yield of solids from the HTL reaction increased with increasing calcium content of the growth media. The yield of the solids from the HTL reaction on algae harvested from tanks 1 and 2 was < 2 dw%.

Over 17 dw% solids were recovered after the HTL reaction on algae harvested from the tank with the highest calcium loading. To further identify if any inorganic solid transformation occurred during the HTL reaction, an inorganic balance was calculated from Eq. (5).

$$\%\text{Inorganic Recovery} = \frac{m_{\text{HTL solids}} \times \%ash_{\text{HTL solids}}}{m_{\text{algae}} \times \%ash_{\text{algae}}} \times 100 \quad (5)$$

where m_{algae} is the mass of algal solids loaded into the reactor, $m_{\text{HTL solids}}$ is the mass of HTL solids recovered from the reactor, $\%\text{ash}_{\text{algae}}$ is the ash wt% of the algal solids and $\%\text{ash}_{\text{HTL solids}}$ is the ash wt% of the HTL solids.

The ash wt% for both the algal and HTL solids was determined using the proximate analysis method on a TGA. Similar to the HTL solids yield and the algal solid ash and calcium content, the recovery of inorganic ash material after HTL were directly related. Only 25–30% of the initial inorganic content of the algal solids from tanks 1 and 2 were recovered in the solid HTL product. Tank 3 algal solids saw a 65% recovery of inorganics in the HTL solids, while algal solids from tanks 4 and 5 had 86% and 82% inorganic recovery in their HTL solids, respectively. Jiang and Savage [35] reported the only substantial amount (> 300 ppm) of metal content present in biocrude from conventional HTL of microalgae to be sodium and iron metals. Thus, the balance of the inorganics, especially those of interest in this study, are expected to be in the ACP. Algal solids harvested from tank 6, however, saw > 130% of the initial inorganic, ash material in the algal solids recovered in the HTL solid product. This indicates a chemical transformation of the inorganic solids occurs during HTL. This transformation causes the mass of solid ash remaining after TGA proximate analysis for the HTL solids to be greater than that of the initial algal solids.

Fig. 2 shows the fate of phosphorus between the ACP and solid HTL products. The phosphorus recovery in the HTL solids was < 72% when the HTL reaction was performed on the algal solid from tanks 1–3. This means that between 28 and 44% of the phosphorus remained in the aqueous phase. The high amount of phosphorus in the aqueous phase is

Table 2
Proximate and inorganic characterization of the algal solids harvested from the six individual light rack tanks.

Tank	Proximate			Inorganic					
	Vol.	Comb.	Ash	Ca	P	Mg	Ca:P	CO_3	XRD
	dw%	*dw%*	*dw%*	*mg/kg*	*mg/kg*	*mg/kg*	*mol*	*wt%*	
1	77.1 ± 0.3	16.8 ± 0.1	6.1 ± 0.3	2490 ± 980	14,180 ± 590	8240 ± 700	0.1	n.d	Amorph.
2	76.3 ± 0.4	17.4 ± 0.1	6.3 ± 0.4	25,700 ± 1500	13,230 ± 530	8.960 ± 630	1.5	3.4	Amorph.
3	77.2 ± 0.3	18.2 ± 0.1	4.6 ± 0.3	50,200 ± 2100	12,630 ± 490	12,380 ± 700	3.1	6.9	Amorph.
4	73.4 ± 0.2	18.6 ± 0.1	8.1 ± 0.1	51,200 ± 2700	11,440 ± 480	7780 ± 690	3.5	8.2	Calcite
5	69.2 ± 0.2	18.6 ± 0.1	12.3 ± 0.2	74,200 ± 2800	10,620 ± 430	9060 ± 610	5.4	11.4	Calcite
6	71.5 ± 0.5	15.4 ± 0.1	13.1 ± 0.5	105,000 ± 3800	10,780 ± 450	8160 ± 600	7.5	15.1	Calcite
		$n = 3$							

Volatiles abrv. Vol.
Combustibles abrv. Comb.
Amorphous abrv. Amorph.
Non-detectable (n.d.)

Table 3
CHNO and macromolecule characterization of the algal solids harvested from the six individual light rack tanks.

Tank	Ultimate				Biochemical		
	C	H	N	O	Carb.	Protein	Lipid*
	dw%	dw%	dw%	dw%	dw%	dw%	dw%
1	53.8 ± 0.1	6.8 ± 0.1	8.9 ± 0.1	20.2 ± 0.3	24.7 ± 3.1	54.2 ± 4.2	9.0
2	53.7 ± 0.1	6.9 ± 0.1	9.1 ± 0.1	20.2 ± 0.1	23.9 ± 2.3	61.4 ± 3.1	9.0
3	53.2 ± 0.1	6.9 ± 0.1	8.9 ± 0.1	20.6 ± 0.2	27.5 ± 3.3	60.9 ± 1.0	8.5
4	50.9 ± 0.1	6.6 ± 0.1	8.3 ± 0.1	20.8 ± 0.2	21.4 ± 2.8	48.8 ± 1.0	7.6
5	47.7 ± 0.1	6.0 ± 0.1	7.7 ± 0.1	20.7 ± 0.2	23.9 ± 5.9	46.9 ± 8.2	8.8
6	46.3 ± 0.1	5.6 ± 0.1	7.4 ± 0.1	21.1 ± 0.3	16.6 ± 4.6	39.4 ± 5.2	7.9
		$n = 3$				$n = 2$	$n = 1$

Carbohydrates abrv. Carb.
* Average std. dev. for lipid analysis was 0.9.

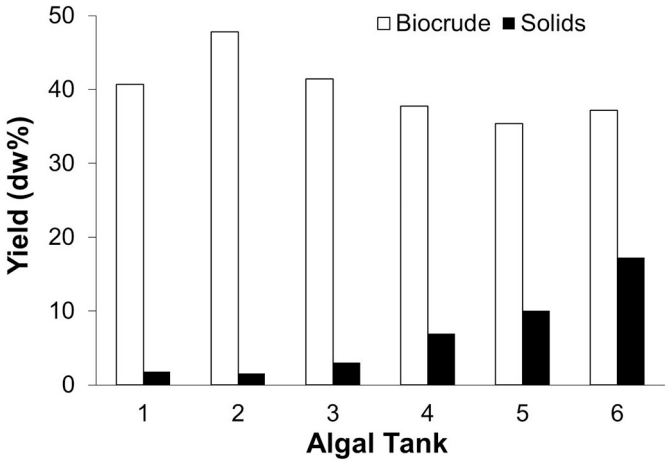

Fig. 1. Biocrude and solids dry weight (dw%) yields from conventional HTL of the six algal solid samples harvested from each individual tank ($n = 1$).

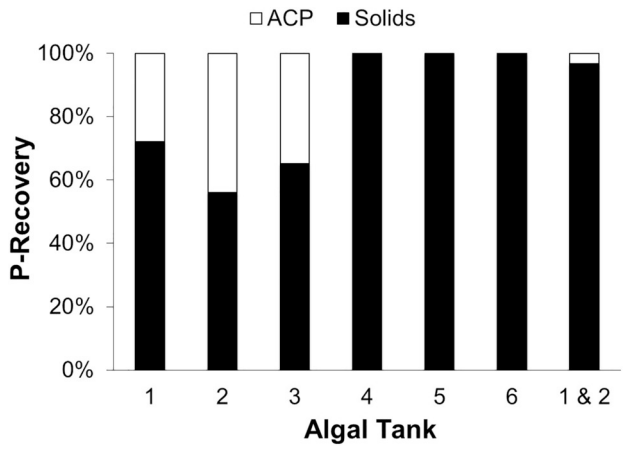

Fig. 2. Phosphorus (P) recovery in the aqueous (ACP) and solid HTL products from individual algal solids harvested from their respective tanks ($n = 3$). An additional HTL reaction was performed combining algal solids from tanks 1 and 2 with $CaCO_3$ to observe its impact on the fate of P post-HTL.

characteristic of many studies previously reported with HTL of single strain, low ash algae [14,15,36]. In contrast to those studies, algal solids from tanks 4–6, saw nearly 100% of the phosphorus retained in the HTL solids. The nearly complete recovery of phosphorus in the HTL solids agree with our previous study from wastewater-cultivated algal solids [12].

The cause for high solid phosphorus recovery could be explained by the higher calcium loading in the growth media. Heilmann et al. demonstrated *via* HTC of various animal manures that manure with higher metal content resulted in higher levels of phosphorus being recovered in the solid product [17]. They suggested this phenomenon was due to formation of highly insoluble, phosphate salts with these metal cations, which is analogous to the observed HAp in the HTL solids from WWAS by Roberts et.al [12,17]. In order to test this hypothesis, an additional HTL reaction was conducted by combining algal solids from tanks 1 and 2 with commercial $CaCO_3$ (Fisher Scientific). An equal mass of algal solids from tanks 1 and 2 were mixed and then doped with 0.2 g of $CaCO_3$. Represented in Fig. 2 as "1 & 2," this reaction resulted in 97% of the phosphorus being recovered in the HTL solids as opposed to the original 72% and 56% of the phosphorus recovered individually from tanks 1 and 2 respectively.

3.3. HTL solids characterization

It is evident that the inorganic species present in the algal solids transform during the HTL reaction. To understand the changes taking place, further characterization of the final solid structure was performed. Fig. 3 depicts the XRD patterns of the solids produced from HTL on the algal solids from tanks 2–6.

The algal solids in these tanks had calcium concentrations ranging from 25,000 mg/L to over 100,000 mg/L, and Ca:P molar ratios > 1.0. The algal solids with low calcium contents (< 2500 and Ca:P molar ratio of 0.1) produced amorphous HTL solids. Peaks associated with crystalline tricalcium phosphate (TCP), $Ca_3(PO_4)_2$, were clearly present in the HTL solids produced from algae harvested from tank 4. Tank 4 had the highest amount of phosphorous in the Pre-Floc media. It is possible that small amounts of TCP are also present in the spectra for the HTL solids from tanks 2, 5, and 6, but no significant peaks were observed. The primary species present in the HTL solids for the algae harvested from tanks 5 and 6 was $CaCO_3$.

Fig. 3 also shows the presence of additional peaks in the XRD that are not characteristic of TCP or $CaCO_3$. We have not yet been able to identify any calcium phosphate or other species that would produce the unidentified peaks. Due to the high probability for substitution in the HTL solid crystalline structure, it is presumed that these HTL solids have acquired additional cations or anions into its crystalline structure making difficult to identify one or multiple, crystalline species. Roberts et al. reported similar substitution in their HTL solids that were primarily, uniform hydroxyapatite, but EDS further showed the presence of Mg and Si [12].

Although XRD did not detect significant crystalline calcium phosphates in all of the HTL solids produced, FTIR experiments provides evidence of the presence of phosphorus and specifically, PO_4^{3-} in the HTL solids. Fig. 4 shows the FTIR spectra of the solids produced from HTL of the algal solids from all six tanks. Phosphate (PO_4^{3-}) has two distinct peaks at 600 and 550 cm^{-1} and a broad peak with multiple

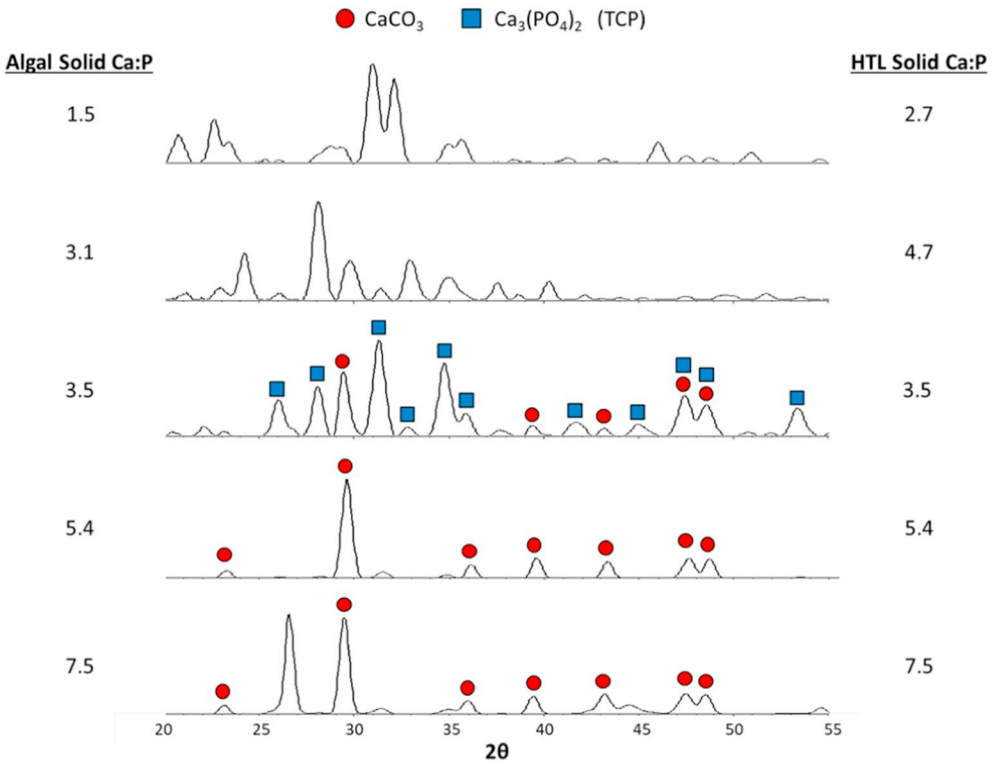

Fig. 3. XRD patterns of the HTL solids produced by algal solids with Ca:P molar ratio between 1.5 and 7.5 shown on the left. The resulting HTL solid Ca:P molar ratio is displayed on the right. Peaks indicative of $CaCO_3$ are shown by circles, while those indicative of TCP are shown by squares.

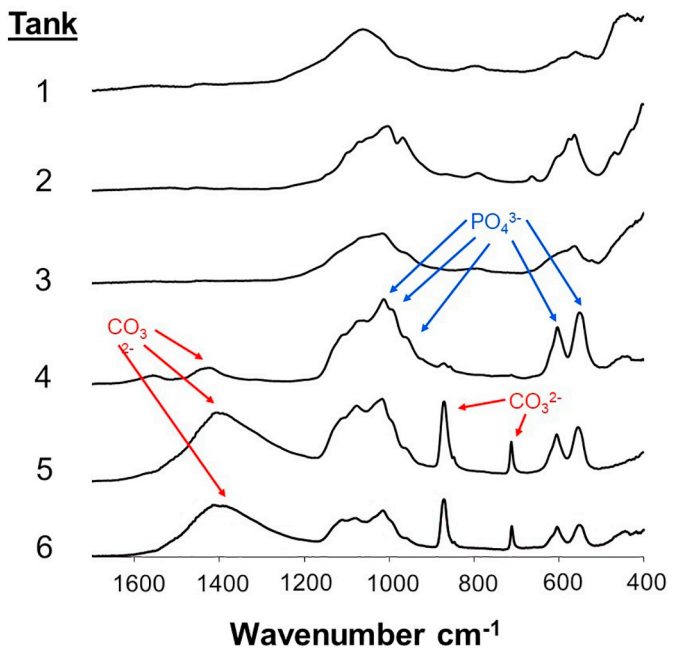

Fig. 4. FTIR spectra of the crystalline HTL solids, which indicate the presence of both CO_3^{2-} and PO_4^{3-} in the HTL solids of high-Ca:P algal solids. The Ca:P molar ratio of the algal solids from Tank 1–6 were 0.1, 1.5, 3.1, 3.4, 5.4, and 7.5, respectively.

shoulders from 900 to 1150 cm^{-1}, which is characteristic of PO_4^{3-} stretching.

All the peaks are clearly present in the HTL solids that were produced from the algal solids harvested from tanks 4–6. In contrast, broad peaks that are not as distinct are observed for the HTL solids produced from the algal solids from tanks 1–3. Carbonate (CO_3^{2-}) peaks typically appear at 712 and 872 cm^{-1} with a broad peak between 1150 and 1650 cm^{-1}. XRD diffraction showed that increasing the calcium content of the growth media resulted in a higher amount of $CaCO_3$ in the algal solids and resulting HTL solids. Fig. 4 confirms the strong presence of carbonate in the HTL solids with the two highest calcium additions but only a small amount in the algae harvested from tank 4. No carbonate was observed in the HTL solid produced from algae harvested from tanks 1–3. Several others have identified the CO_3^{2-} and PO_4^{3-} peaks to be characteristic of substituted apatites and TCP minerals similar to what is observed in these HTL solids [12,27,37,38].

XRD and FTIR provide qualitative results and are not as accurate for quantitative analysis. Thus, alternative methods were used to further quantify the carbonate and phosphate in the HTL solids. Fig. 5 depicts the derivative weight curves for the six solid samples produced from HTL. In addition, the derivative weight curve for pure calcium carbonate is also shown. The change in weight between 600 and 800 °C is due to the loss of CO_2 during the decomposition of $CaCO_3$ to CaO [39]. Analysis of the pure $CaCO_3$ data proves that the wt% of carbonate in the sample can be accurately determined from the measured CO_2 weight loss. HTL solids produced from algal solids from tanks 1–3 had negligible amounts of carbonate. In contrast, the solids produced from HTL of algae harvested from tanks 4–6 contained significant amount of carbonate as shown in Table 4. The amount of carbonate was found to range from near 3% to 41% with higher calcium loadings resulting in higher carbonate percentages in the HTL solids.

With the initial carbonate at most being 15 wt% for the algal solid samples, it appears that the HTL solids gained carbonate mass during the reaction. In terms of recovery, HTL solids with the highest calcium contents had > 100% carbonate recovery. The increase in carbonate could be caused by the excess Ca^{2+} cations bonding with bicarbonate (HCO_3^-) during the HTL reaction. Bicarbonate will form during HTL from the interaction of CO_2 gas that is produced by decomposition of the algal biomolecules and water. The *in-situ* generation of $CaCO_3$ could also explain the higher inorganic recovery also seen at the high Ca:P molar ratio.

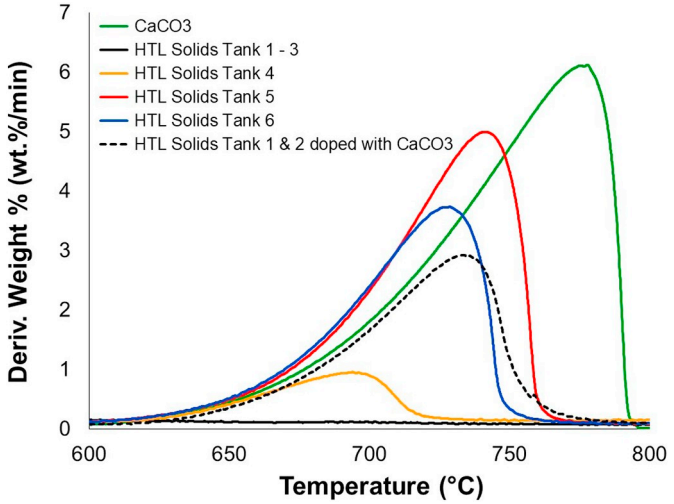

Fig. 5. Thermogravimetric analysis derivative weight curves of $CaCO_3$ for reference and the six HTL solid samples produced by the algal solids with varying calcium concentration in the growth media. The dashed black line represents the derivative weight curve of for the HTL solids produced from a 50/50 mixture of algal solids from tank 1 and 2 doped with $CaCO_3$.

Although the exact role of the calcium and carbonate in facilitating phosphorus recovery are not clear, the data suggests that the amount of carbonate in the HTL solids may be important. Comparing the results in tank 3 and tank 4, the calcium concentrations and Ca:P molar ratio in the algal solids are similar. However, a large difference in the carbonate content of the HTL solids is observed corresponding to an increase in phosphorus recovery of over 35%. The phosphorus recovery in tanks 4–6 reached nearly 100% and the HTL solids from these runs also showed quantifiable amounts of carbonate according to the FTIR, XRD, and TGA data. Finally, the doping of $CaCO_3$ to a mixture of algae harvested from tanks 1 and 2, clearly shows an increase in phosphorus recovery. It should be noted that the amount of $CaCO_3$ added to the mixture would have made the Ca:P ratio equivalent to 2.4. Thus, it would be expected that if the recovery were based solely on Ca:P ratio or calcium content that the recovery would be similar to what was measured with the experiments on the algal solids harvested from tanks 2 and 3. Additional studies are necessary to determine the exact role of the calcium and carbonate in the phosphorus recovery.

3.4. Biocrude characterization

The CHNO composition and the HHV for the biocrude are also shown in Table 4. Comparison of the distillate fractions for the various samples in the study indicates that the different calcium loadings in the growth media did not significantly impact HHV (37–41 MJ/kg) or the boiling point distribution for the biocrude produced. The most abundant distillation fraction for all Ca:P molar ratios was that of the vacuum gas fraction (343–538 °C) at 35.7 ± 4.8 wt%, followed by kerosene (193–271 °C) at 21.8 ± 2.8 wt% and vacuum residual (> 538 °C) fractions at 19.3 ± 1.5 wt%. The least abundant fractions were the gasoline (271–343 °C) and heavy naphtha fraction (< 193 °C) at 10.8 ± 2.2 wt% and 11.6 ± 1.1 wt%, respectively. The distribution and range for the given distillation fractions is similar to what we have previously reported for HTL on wastewater cultivated algae [12]. In addition, 90 wt% or higher of the biocrude distilled off by 600 °C. By comparison, Chen et al. observed approximately 16–32 wt% residual in the simulated distillation of their biocrude product at 600 °C [6,13]. Similarly, Roussis et al. [40] observed only 77% of their initial HTL biocrude to be distilled off by 550 °C. It was not until after a 450 °C secondary thermal treatment that their biocrude product showed similar distillate properties to the biocrude fractions in this study. Biocrude products that have a greater amount of light distillate fractions, such as those that appear in this study, are more desirable because less refining and upgrading is required for the product to be used in existing infrastructure.

The carbon content of the biocrude produced from HTL on the algal solids from all the tanks was near 79%. Similarly, no significant variation was observed in the nitrogen content (average 5.4%). The average oxygen content was 6.5% with the biocrude produced from HTL of the algal solids from tank 5 being slightly lower at 5.7%. The hydrogen content ranged from 8.7% to 10.6% with the biocrude produced from the algal solids harvested from tank 2 and 3 being over 10%. The N/C and O/C ratios were both close to 0.06 regardless of the growth conditions. This range of O/C and N/C are typical for HTL biocrude from algae where the ACP was separated prior to the addition of extraction solvent (DCM) [12,41,42]. Comparison of the H/C ratio for the biocrudes produced from the different algal solids is shown in Fig. 6. The H/C ratio varied from 1.31 to 1.59 with the lowest H/C ratio produced at the lowest and highest calcium additions to the growth media. While there appears to be no obvious trend between the calcium addition or Ca:P ratio of the algal solids and the H/C ratio of the biocrude, the analysis of the doping of $CaCO_3$ to a mixture of the algal solids from tank 1 and 2 may provide some explanation.

When $CaCO_3$ was added doped into the reactor, the highest biocrude H/C of 1.65 was achieved. Thus, the $CaCO_3$ observed in the algal solids may be having an *in-situ* catalytic effect on the biocrude. Jena et al. saw a similar increase in the H/C ratio as well as the highest C and H recovery in the biocrude from HTL reactions that were doped with Na_2CO_3. They hypothesized that at the subcritical water conditions of HTL and in the presence of algal macromolecules Na_2CO_3 reacts to form sodium formate. Through a subsequent series of reactions OH^- and $HCOO^-$ ions are created, which further decompose the algal hydrocarbon macromolecules to the biocrude product [43]. A similar phenomena could also be occurring from the addition and presence of $CaCO_3$ in the algal solids.

A key difference between the potential, *in-situ*, $CaCO_3$ catalysis observed in this study and the common alkali metal carbonate salt Na_2CO_3

Table 4
Properties of the biocrude, aqueous co-product (ACP), and HTL solids.

Tank	Biocrude					ACP					HTL Solids	
	C	H	N	O	HHV	Aq. C	Aq. N	Ca	P	Mg	Ash	CO_3
	wt%	wt%	wt%	wt%	MJ/kg	%	%	mg/L	mg/L	mg/L	wt%	wt%
1	79.3 ± 0.8	8.7 ± 0.2	5.7 ± 0.1	7.0 ± 0.3	37.9 ± 0.9	15.4 ± 0.1	54.4 ± 0.1	1.2 ± 0.1	461 ± 5	0.1 ± 0.1	53.1	2.7
2	80.0 ± 0.8	10.2 ± 0.1	5.1 ± 0.1	6.5 ± 0.2	40.4 ± 0.9	17.8 ± 0.1	55.7 ± 0.2	0.2 ± 0.1	649 ± 5	0.1 ± 0.1	57.9	2.8
3	79.6 ± 0.4	10.6 ± 0.2	5.4 ± 0.1	6.7 ± 0.1	40.7 ± 0.5	15.9 ± 0.1	60.2 ± 0.1	0.2 ± 0.1	506 ± 2	0.3 ± 0.1	58.6	2.9
4	78.2 ± 0.4	9.4 ± 0.1	5.3 ± 0.1	6.5 ± 0.2	38.6 ± 0.5	16.5 ± 0.1	62.7 ± 0.1	0.7 ± 0.1	1.0 ± 0.1	1.2 ± 0.1	71.8	8.0
5	78.3 ± 0.9	9.8 ± 0.1	5.3 ± 0.1	5.7 ± 0.1	39.3 ± 1.0	17.5 ± 0.1	61.5 ± 0.1	0.7 ± 0.1	3.6 ± 0.1	7.5 ± 0.1	59.8	41.1
6	78.6 ± 1.1	8.8 ± 0.4	5.4 ± 0.1	6.9 ± 0.2	37.8 ± 1.2	15.2 ± 0.1	61.3 ± 0.1	1.0 ± 0.1	1.7 ± 0.1	0.1 ± 0.1	68.7	30.5
	$n = 3$					$n = 3$			$n = 3$		$n = 1$	

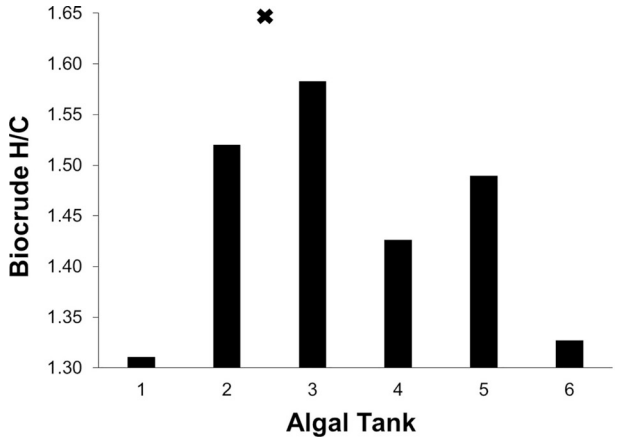

Fig. 6. Biocrude H/C atom ratios from the varying Ca:P algal solids harvested from each individual tank. The "X" represents the H/C biocrude ratio from HTL reaction of lower Ca:P algal solids from tank 1 and 2 that were doped with $CaCO_3$. The uncertainty in the H/C ratio (n = 3) for all tanks was ± 0.02 except tank 1 (± 0.03) and tank 6 (± 0.05).

is that $CaCO_3$ is significantly more insoluble in water (6.17×10^{-4} g/100 mL water at 20 °C) than the Na_2CO_3 (21.5 g/100 mL). Thus, the dissociation of $CaCO_3$ is most likely the rate-limiting step in the possible *in-situ* catalysis of the biocrude oil. However, Coto et al. demonstrated that, while the solubility of $CaCO_3$ decreases with higher temperatures, it dramatically increases with higher pressures of CO_2 and presence of other ions [44]. Thus, the presence of the other inorganic ions and high pressure CO_2 that is known to be produced by the organic, biomolecules of algal biomass, can promote $CaCO_3$ dissociation and *in-situ* catalysis. Chen et al. suggested that the carbonate ion formed from $CaCO_3$ dissociation can react with ammonia produced from the degradation of proteins to from ammonium carbonate. The ammonium carbonate would degrade to carbon dioxide, water, and gaseous ammonia effectively lowering the N content of the biocrude, ACP and solid product. They also suggested that the carbonate ion could react with water to form bicarbonates, which can catalyze the water-gas shift reaction [13]. While CO_3^{2-} may be impacting the biocrude, the higher availability Ca^{2+} has been shown to be the initial nucleation step for the hydrothermal synthesis of calcium phosphates, such as HAp [45] and, thus, is also believed to impact the phosphorus recovery in the HTL solids.

3.5. Biocrude composition

GC–MS of the HTL biocrude further depicts the role that the inorganic content of algal solids may have *in-situ* on the HTL biocrude product. Table 5 reports the summation of the percent area for peaks in four categories: aliphatics, aromatics, nitrogen-, and oxygen-compounds. Aliphatics were alkanes, alkenes, and derivatives of alkanes and alkenes. The primary aromatic compounds included benzene derivatives, phenol, phenol derivatives, p-cresol, styrene, and naphthalene derivatives. Included in the nitrogen compounds were amide, indole, indole derivatives, pyrazine derivative, pyrrole, pyridine, quinolone derivatives, and pyrrolidinone derivatives. Finally, the primary oxygen containing compounds were hexadecanoic acid, octadecanoic acid, cyclic ketone, and alcohols. The relative peak areas of the various compounds provides a comparison in the biocrude composition produced from the HTL reaction of the six distinct algal solids. In all the biocrude samples, the aromatics were lower than any other category and were primarily phenol, phenol derivatives, and naphthalene derivatives. For the aliphatic compounds, hexadecene derivatives were by far the most abundant compound present in the biocrude. Hexadecanoic acid and octadecanoic acid accounted for the majority of the oxygen compounds. In the tanks with lower calcium contents (tank 1–3) the amount of hexadecanoic acid was much higher than the amount of octadecanoic acid. Increasing the calcium content resulted in an increase in the octadecanoic acid content and in the biocrude produced from algal solids harvested from tanks 4 and 5, more octadecanoic acid production than hexadecanoic acid.

Another interesting observation is in the nitrogen containing compounds, specifically the amide species. The biocrude produced from algal solids harvested from tank 4–6 have significant less amide compounds than the biocrude from the other algal solids. This reduction in amides could be due to the reduction in the protein content of the algal solids as shown in Table 3. However, when $CaCO_3$ was doped with the low calcium containing algal solids from tank 1 and 2, the amide concentration of the resulting biocrude was again low, even though the protein content of the starting algae was high. This biocrude also had a lower carboxylic acid content, 9.92%, compared to the biocrude produced from the algae harvested from tank 1 and tank 2 at 16.25% and 12.63%, respectively. Biller and Ross did notice a higher conversion of lipid compounds to alkenes with the addition of Na_2CO_3 [9] and also showed that Na_2CO_3 had the most success of converting carbohydrates to biocrude compounds. Jena et al. saw an increase in the carboxylic acid abundance in the biocrude from the addition of Na_2CO_3 [43]. However, R. Shakya reported lower organic acid yields in the biocrude with the addition of Na_2CO_3 [46]. The decrease in amide and acid content further shows the potential *in-situ* biocrude enhancement $CaCO_3$ may have during the HTL reaction. As previously stated, the high partial pressures of CO_2 in the HTL reactor could increase the solubility of $CaCO_3$ during the HTL reaction [44]. The increased solubility could lead to the changes in the CHNO distribution in the products either through solubility changes or through reactions facilitated by Ca^{2+} and/or CO_3^{2-} [13,43,46]. Thus, the presence of $CaCO_3$ captured during harvesting could explain the similarities in biocrude yield and the positive impact on the biocrude properties compared to other low ash, low HTL solids yielding algae.

Table 5
Commonly identified HTL biocrude compounds and their relative peak areas from algal solids with varied Ca:P ratios (n = 1).

Tank	Ca:P Molar Ratio in Algal Solids	CO_3 wt% in Algal Solids	CO_3 wt% in HTL Solids	Aliphatics	Aromatics	Nitrogen Compounds	Oxygen Compounds
1	0.1	n.d.	2.7	20.64	8.99	16.08	18.58
2	1.5	3.4	2.8	16.33	6.47	16.47	13.72
3	3.1	6.9	2.9	22.91	8.68	18.46	8.29
4	3.5	8.2	8.0	16.28	6.70	12.46	18.72
5	5.4	11.4	41.1	12.44	4.62	14.87	11.80
6	7.5	15.1	30.5	16.09	8.72	13.64	18.70
50/50 Mixture Tank 1 & 2 Doped with $CaCO_3$	2.4	25.36	25.5	18.39	10.74	13.41	12.53

Non-detectable (n.d.)

4. Conclusions

Increasing the calcium concentration of the algal growth media does not have a large impact on the ultimate and biochemical content of the algae. Lower protein content was observed with higher calcium concentration due to small amounts of phosphorus precipitation in the growth media. When harvested at a high pH, various calcium and phosphorus species precipitate out of the algal media increasing the calcium, phosphorus, and ash wt% of the algal solids. Calcium carbonate was the primary crystalline structure observed in the algal solids with higher calcium contents; however, other amorphous calcium phosphate species are also suspected to be present. The greater presence of inorganics had a large impact on the HTL solids. The fate of phosphorus in the products shifted from the ACP to the HTL solids at higher calcium loadings in the growth media. The higher calcium concentrations resulted in near 100% capture of phosphorus in the HTL solids. In addition, the formation of TCP, $CaCO_3$, and substituted forms of calcium phosphates and $CaCO_3$ were observed in the HTL solids. Increasing the calcium content also had a positive impact on the biocrude, including the H/C ratio, amide, alkene, and carboxylic acid content. The results of this study suggest that the inorganic solids collected from high pH, flocculated, harvesting may have an *in-situ* catalytic impact on the biocrude.

Contribution declaration and conflict of interest

This manuscript reports new findings and is not under consideration elsewhere. All co-authors agree with the submission of this manuscript.

Susan M Stagg Williams is responsible for obtaining funding, conception and design, critical revision of the article for important intellectual content, and final approval of the article.

Robert D Hable is responsible for conception and design, collection and assembly of data, analysis and interpretation of the data, drafting of the article.

Sirwan Alimoradi is responsible for conception and design, collection and assembly of data, analysis and interpretation of the data, critical revision of the article for important intellectual content.

Belinda SM Sturm is responsible for obtaining funding, conception and design, critical revision of the article for important intellectual content.

Funding

This work was supported by the National Science Foundation (NSF CBET-1438652).

References

[1] B.K. Mayer, L.A. Baker, T.H. Boyer, P. Drechsel, M. Gifford, M.A. Hanjra, P. Parameswaran, J. Stoltzfus, P. Westerhoff, B.E. Rittmann, Total value of phosphorus recovery, Environ. Sci. Technol. 50 (13) (2016) 6606–6620.
[2] A. Mehrabadi, R. Craggs, M.M. Farid, Wastewater treatment high rate algal pond biomass for bio-crude oil production, Bioresour. Technol. 224 (2017) 255–264.
[3] G.W. Roberts, M.-O.P. Fortier, B.S.M. Sturm, S.M. Stagg-Williams, Promising pathway for algal biofuels through wastewater cultivation and hydrothermal conversion, Energy Fuel 27 (2) (2013) 857–867.
[4] B.S.M. Sturm, S.L. Lamer, An energy evaluation of coupling nutrient removal from wastewater with algal biomass production, Appl. Energy 88 (10) (2011) 3499–3506.
[5] M.-O. Fortier, B.S.M. Sturm, Geographic analysis of the feasibility of collocating algal biomass production with wastewater treatment plants, Environ. Sci. Technol. 46 (20) (2012) 11426–11434.
[6] W.T. Chen, Y. Zhang, J. Zhang, G. Yu, L.C. Schideman, P. Zhang, M. Minarick, Hydrothermal liquefaction of mixed-culture algal biomass from wastewater treatment system into bio-crude oil, Bioresour. Technol. 152 (2014) 130–139.
[7] J.M. Jarvis, J.M. Billing, R.T. Hallen, A.J. Schmidt, T.M. Schaub, Hydrothermal liquefaction biocrude compositions compared to petroleum crude and shale oil, Energy Fuel 31 (3) (2017) 2896–2906.
[8] U. Jena, K.C. Das, J.R. Kastner, Effect of operating conditions of thermochemical liquefaction on biocrude production from Spirulina platensis, Bioresour. Technol. 102 (10) (2011) 6221–6229.
[9] P. Biller, A.B. Ross, Potential yields and properties of oil from the hydrothermal liquefaction of microalgae with different biochemical content, Bioresour. Technol. 102 (1) (2011) 215–225.
[10] K. Anastasakis, A.B. Ross, Hydrothermal liquefaction of the brown macro-alga Laminaria saccharina: effect of reaction conditions on product distribution and composition, Bioresour. Technol. 102 (7) (2011) 4876–4883.
[11] S.S. Toor, L. Rosendahl, A. Rudolf, Hydrothermal liquefaction of biomass: a review of subcritical water technologies, Energy 36 (5) (2011) 2328–2342.
[12] G.W. Roberts, B.S.M. Sturm, U. Hamdeh, G.E. Stanton, A. Rocha, T.L. Kinsella, M.-O.P. Fortier, S. Sazdar, M.S. Detamore, S.M. Stagg-Williams, Promoting catalysis and high-value product streams by in situ hydroxyapatite crystallization during hydrothermal liquefaction of microalgae cultivated with reclaimed nutrients, Green Chem. 17 (4) (2015) 2560–2569.
[13] W.-T. Chen, W. Qian, Y. Zhang, Z. Mazur, C.-T. Kuo, K. Scheppe, L.C. Schideman, B.K. Sharma, Effect of ash on hydrothermal liquefaction of high-ash content algal biomass, Algal Res. 25 (2017) 297–306.
[14] P. Biller, A.B. Ross, S.C. Skill, A. Lea-Langton, B. Balasundaram, C. Hall, R. Riley, C.A. Llewellyn, Nutrient recycling of aqueous phase for microalgae cultivation from the hydrothermal liquefaction process, Algal Res. 1 (1) (2012) 70–76.
[15] U. Ekpo, A.B. Ross, M.A. Camargo-Valero, P.T. Williams, A comparison of product yields and inorganic content in process streams following thermal hydrolysis and hydrothermal processing of microalgae, manure and digestate, Bioresour. Technol. 200 (2016) 951–960.
[16] G. Yu, Y. Zhang, B. Guo, T. Funk, L. Schideman, Nutrient flows and quality of biocrude oil produced via catalytic hydrothermal liquefaction of low-lipid microalgae, BioEnergy Res. 7 (4) (2014) 1317–1328.
[17] S.M. Heilmann, J.S. Molde, J.G. Timler, B.M. Wood, A.L. Mikula, G.V. Vozhdayev, E.C. Colosky, K.A. Spokas, K.J. Valentas, Phosphorus reclamation through hydrothermal carbonization of animal manures, Environ. Sci. Technol. 48 (17) (2014) 10323–10329.
[18] C. Dayananda, R. Sarada, M. Usharani, T. Shamala, G. Ravishankar, Autotrophic cultivation of Botryococcus braunii for the production of hydrocarbons and exopolysaccharides in various media, Biomass Bioenergy 31 (1) (2007) 87–93.
[19] S. Leow, J.R. Witter, D.R. Vardon, B.K. Sharma, J.S. Guest, T.J. Strathmann, Prediction of microalgae hydrothermal liquefaction products from feedstock biochemical composition, Green Chem. 17 (6) (2015) 3584–3599.
[20] D. Vandamme, I. Foubert, K. Muylaert, Flocculation as a low-cost method for harvesting microalgae for bulk biomass production, Trends Biotechnol. 31 (4) (2013) 233–239.
[21] A.I. Barros, A.L. Gonçalves, M. Simões, J.C.M. Pires, Harvesting techniques applied to microalgae: a review, Renew. Sust. Energ. Rev. 41 (2015) 1489–1500.
[22] W.D. Davidson, M.A. Sackner, Simplification of the anthrone method for the determination of inulin in clearance studies, Transl. Res. 62 (2) (1963) 351–356.
[23] E.F. Hartree, Determination of protein: a modification of the Lowry method that gives a linear photometric response, Anal. Biochem. 48 (2) (1972) 422–427.
[24] B.M. Barney, B.D. Wahlen, E. Garner, J. Wei, L.C. Seefeldt, Differences in substrate specificities of five bacterial wax ester synthases, Appl. Environ. Microbiol. 78 (16) (2012) 5734–5745.
[25] L.M. Laurens, M. Quinn, S. Van Wychen, D.W. Templeton, E.J. Wolfrum, Accurate and reliable quantification of total microalgal fuel potential as fatty acid methyl esters by in situ transesterification, Anal. Bioanal. Chem. 403 (1) (2012) 167–178.
[26] B.S. Sturm, E. Peltier, V. Smith, F. deNoyelles, Controls of microalgal biomass and lipid production in municipal wastewater-fed bioreactors, Environ. Prog. Sustain. Energy 31 (1) (2012) 10–16.
[27] K. Ishikawa, S. Matsuya, X. Lin, Z. Lei, T. Yuasa, Y. Miyamoto, Fabrication of low crystalline B-type carbonate apatite block from low crystalline calcite block, J. Ceram. Soc. Jpn. 118 (5) (2010) 341–344.
[28] J. Jiang, P.E. Savage, Metals and other elements in biocrude from fast and isothermal hydrothermal liquefaction of microalgae, Energy Fuel 32 (4) (2018) 4418–4426.
[29] D. Vandamme, I. Foubert, I. Fraeye, B. Meesschaert, K. Muylaert, Flocculation of Chlorella vulgaris induced by high pH: role of magnesium and calcium and practical implications, Bioresour. Technol. 105 (2012) 114–119.
[30] Y. Song, H.H. Hahn, E. Hoffmann, Effects of solution conditions on the precipitation of phosphate for recovery: a thermodynamic evaluation, Chemosphere 48 (10) (2002) 1029–1034.
[31] V.H. Smith, B.S. Sturm, S.A. Billings, The ecology of algal biodiesel production, Trends Ecol. Evol. 25 (5) (2010) 301–309.
[32] A.C. Redfield, The biological control of chemical factors in the environment, Am. Sci. 46 (3) (1958) 230A–221.
[33] G.Y. Rhee, Effects of N: P atomic ratios and nitrate limitation on algal growth, cell composition, and nitrate uptake 1, Limnol. Oceanogr. 23 (1) (1978) 10–25.
[34] T.M. Brown, P. Duan, P.E. Savage, Hydrothermal liquefaction and gasification of Nannochloropsis sp, Energy Fuel 24 (6) (2010) 3639–3646.
[35] J. Jiang, P.E. Savage, Influence of process conditions and interventions on metals content in biocrude from hydrothermal liquefaction of microalgae, Algal Res. 26 (2017) 131–134.
[36] L. Zhang, H. Lu, Y. Zhang, B. Li, Z. Liu, N. Duan, M. Liu, Nutrient recovery and biomass production by cultivating Chlorella vulgaris 1067 from four types of post-hydrothermal liquefaction wastewater, J. Appl. Phycol. 28 (2) (2015) 1031–1039.
[37] M. Kamitakahara, T. Nagamori, T. Yokoi, K. Ioku, Carbonate-containing hydroxyapatite synthesized by the hydrothermal treatment of different calcium carbonates in a phosphate-containing solution, J. Asian Ceramic Soc. 3 (3) (2015) 287–291.
[38] T. Arahira, M. Maruta, S. Matsuya, Development and characterization of carbonate apatite/β-tricalcium phosphate biphasic cement, Mater. Lett. 194 (2017) 205–208.

[39] C. Rodriguez-Navarro, E. Ruiz-Agudo, A. Luque, A.B.R.-N.M. Ortega-Huertas, Thermal decomposition of calcite: mechanisms of formation and textural evolution of CaO nanocrystals, Am. Mineral. 94 (4) (2009) 578–593.
[40] S.G. Roussis, R. Cranford, N. Sytkovetskiy, Thermal treatment of crude algae oils prepared under hydrothermal extraction conditions, Energy Fuel 26 (8) (2012) 5294–5299.
[41] D. Xu, P.E. Savage, Characterization of biocrudes recovered with and without solvent after hydrothermal liquefaction of algae, Algal Res. 6 (2014) 1–7.
[42] D. Xu, P.E. Savage, Effect of reaction time and algae loading on water-soluble and insoluble biocrude fractions from hydrothermal liquefaction of algae, Algal Res. 12 (2015) 60–67.
[43] U. Jena, K.C. Das, J.R. Kastner, Comparison of the effects of Na_2CO_3, $Ca_3(PO_4)_2$, and NiO catalysts on the thermochemical liquefaction of microalga Spirulina platensis, Appl. Energy 98 (2012) 368–375.
[44] B. Coto, C. Martos, J.L. Peña, R. Rodríguez, G. Pastor, Effects in the solubility of $CaCO_3$: experimental study and model description, Fluid Phase Equilib. 324 (2012) 1–7.
[45] M. Sadat-Shojai, M.T. Khorasani, E. Dinpanah-Khoshdargi, A. Jamshidi, Synthesis methods for nanosized hydroxyapatite with diverse structures, Acta Biomater. 9 (8) (2013) 7591–7621.
[46] R. Shakya, J. Whelen, S. Adhikari, R. Mahadevan, S. Neupane, Effect of temperature and Na_2CO_3 catalyst on hydrothermal liquefaction of algae, Algal Res. 12 (2015) 80–90.